Formability and Accuracy of Micropolymer Compound with Added Nanomaterials in Microinjection Molding

C. K. Huang, S. W. Chiu

Department of Mechanical Engineering, Lunghwa University of Science and Technology, 300 Wan-Shou Road Section 1, Kueishan, Taoyuan, Taiwan, Republic of China

Received 26 January 2005; accepted 18 March 2005
DOI 10.1002/app.21927
Published online in Wiley InterScience (www.interscience.wiley.com).

ABSTRACT: The miniaturization of components has been progressing rapidly because of developments in microelectronics, optoelectronics, and biotechnology. Recently, the use of plastic materials with added fillers has become a potential alternative because of their versatility and ease of batch fabrication. This article investigates the formability and accuracy of the polymer with added nanopowders (10–30 nm diameter) during microinjection molding. One mold with four cavities is used to illustrate the filling behavior and accuracy of the microparts. The integrated circuit microfeature illustrates the formability of the polymer with added nanopowders. Experiments show that the shrinkage is significantly reduced when the nanopowder content is increased. The polymer with 30% ZnO nanopowder content shows 58.3% less shrinkage compared to pure polypropylene. One mold with four parts and the microfeature are successfully manufactured using a custom-made microinjection machine when nanopowders are added to the polymer. However, the microfeature with added fillers, which had a diameter of 10 μm and a length of 10–30 μm, cannot be duplicated through microinjection molding. © 2005 Wiley Periodicals, Inc. J Appl Polym Sci 98: 1865–1874, 2005

Key words: nanomaterial; micropart; microinjection molding; microinjection machine; shrinkage; fillers

INTRODUCTION

Microsystem technology has been applied in the fluidic, medical, optical, and telecommunication fields. To exploit the potential of microsystem technology, economical mass production of microcomponents is necessary.[1,2] Most of the components for miniaturized systems have been fabricated using silicon, glass, or quartz. However, for many applications, these materials and the associated fabrication methods are too expensive and complicated.[3,4] Recently, the use of plastic materials has become a potential alternative because of their versatility and ease of batch fabrication.[5,6] Among a variety of polymer processing methods, microinjection molding is one of the most suitable processes for replicating microparts (even those with microstructures) cheaply and with high precision.[7–9]

Kukla et al.[10] defined microinjection molded parts as parts with microweights, parts with microstructured regions, and parts with microprecision dimensions. Parts with microweights are parts with masses of a few milligrams, but their dimensions are not necessarily on the micron scale. Parts with microstructured regions are characterized by local microfeatures on the order of microns, such as the microhole and slot. Parts with microprecision are parts of any dimension, but they have tolerances in the micron range. This article focuses on the first and second categories. That is, the molding of microparts with weights is on the order of $<$3 mg and microregions are on the order of a few microns.

A number of pure plastics, for example, liquid crystalline polymers, polycarbonate, polystyrene, polypropylene (PP), poly(methyl methacrylate), and polyoxymethylene, or, acetal (POM), have been successfully processed through the micromolding process.[11–14] However, most microparts, such as gears and fans, require high strength, wear resistance, and accuracy. However, plastic materials cannot satisfy these requirements. Some researchers[15–19] have produced microparts through micropowder injection molding. This technique includes blending, molding, debinding, and sintering processes. In addition to taking time, cracks in and high shrinkage of microparts easily occur with this technique, although high strength and wear resistance can be obtained.

Schneider and Maier[20] added fillers to plastics to reinforce their structures and reduce shrinkage. However, these fillers cannot be used successfully in the micromolding process. This is because the compound component and the fillers, such as glass fibers with a

Correspondence to: C. K. Huang (ckhuang@mail.me.lhu.edu.tw).

Contract grant sponsor: National Science Council of Taiwan; contract grant number: NSC92-2212-E-262-006.

© 2005 Wiley Periodicals, Inc.

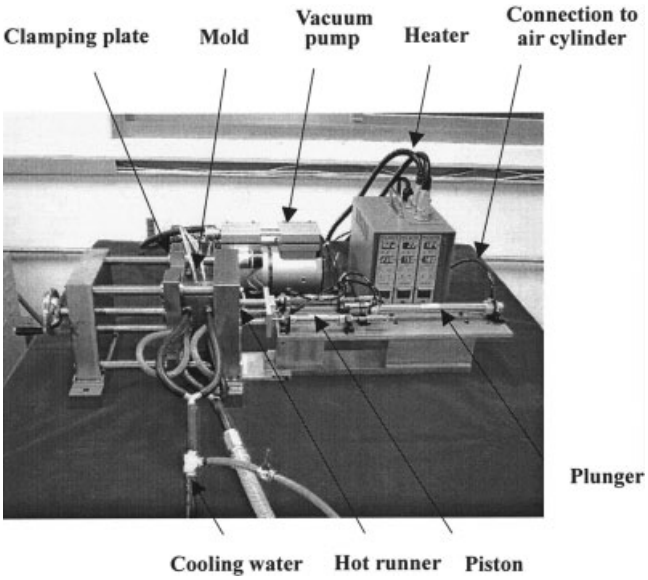

Figure 1 The custom-made microinjection machine.

typical diameter of 10 μm and a length of 100–500 μm, are often as big as some of the microparts to be molded. Thus, microparts with added nanomaterials (10–30 nm diameter) could possibly be used in microinjection molding.

Strength, wear resistance, accuracy, and filling properties are the key factors involved the manufacturing of quality microparts. This article mainly discusses the application of nanomaterials in microinjection molding. Nanomaterials were added into a polymer to observe the filling properties of the parts. Under batch production, high quality microparts can be manufactured only when the filling parameters are well controlled. Thus, this study focused on the filling properties and accuracy of the microparts.

One mold with four cavities and an integrated circuit (IC) chip with microregions were used as to study filling behavior and accuracy in microinjection molding. Nanomaterials (10–30 nm diameter), such as SiO_2, TiO_2, and ZnO, were introduced into PP polymer to reduce shrinkage and observe the filling behavior of the microparts during microinjection molding. All tests were conducted in a custom-made microinjection machine.

EXPERIMENTAL

Custom-made injection machine and processing window

The parts tested in this study were formed using a custom-made microinjection machine. Figure 1 shows the custom-made impact type microinjection machine, which cost only U.S. $2,000 to construct. In addition to saving money, it also has many functions, making it suitable for various kinds of tests.

This machine mainly includes clamping, melting, and injection units. The movable and fixing plates are fixed on the clamping device; therefore, it can move forward and backward under pressure exerted by rotating a hand wheel on the device. The mold is locked on a fixing plate with bolts. The melt unit mainly uses a hot runner to provide plastic melting energy. Inside the hot runner, there is an injection sleeve with a 2-mm diameter hole, which serves as the barrel of the microinjection machine. The injection unit mainly includes the injection plunger and an air cylinder. The injection plunger is used to push the molten polymer into the mold cavity. A vacuum pump is used to remove air or waste gas during forming. The maximum shot and injection pressure of this machine are 120 mm^3 and 7 bar, respectively. The permissible mold and melt temperatures are 200 and 300°C, respectively. The clamping force of the mold is 750 N.

The processing window is an effective tool for finding the range of processing parameters for quality parts. In this experiment, the injection pressure and the mold temperature are significant processing parameters. The melt temperature is a minor factor in the production of small parts when compared to the other two parameters.[21,22] Thus, we kept the melt temperature at a constant 220°C to find the processing window. The injection pressure and the mold temperature were varied point by point to find the processing window. Short-shot or flash in parts is located outside the boundary of the processing window. The permissible injection pressure, called the mechanical ability, cannot exceed 7 bar in this window.

Materials and methods

Materials and specimens

The raw materials used in the study included nanoceramic materials (NCM), PP, and stearic acid (SA). Three kinds of NCMs (SiO_2, TiO_2, and ZnO) with diameters of 10–30 nm were used as parts fillers and were made by the Z-Tech Co. PP (Formosa Plastic) was used as a backbone polymer matrix. SA (Nacalai Tesque) acted as a surfactant for the ceramic and polymeric ingredients. The polymeric ingredients had NCM/PP/SA weight ratios of 10 : 89 : 1, 20 : 78 : 2, and 30 : 67 : 3.

One mold with four cavities of slightly varying dimensions was used to study the filling behavior and accuracy in batch fabrication tests, as shown in Figure 2. Following duplication, the dimensions of each part and its corresponding cavity were compared. To understand the formability of the microfeatures with added nanopowders, the boundaries of a weld spot (8.54 $\times$ 18.75 μm) in an IC chip, which was taken from a scraped computer, were duplicated, as shown in Figure 3. Residual adhesive was deposited in the cen-

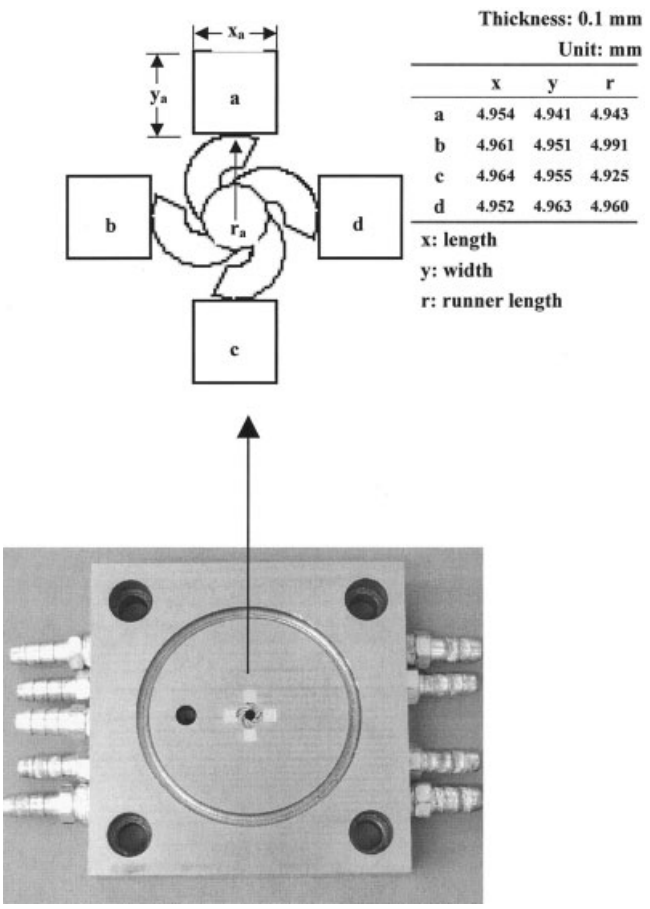

	x	y	r
a	4.954	4.941	4.943
b	4.961	4.951	4.991
c	4.964	4.955	4.925
d	4.952	4.963	4.960

Figure 2 The measured lengths of the mold with four cavities.

ter of the weld spot because it was difficult to clean out. In addition, the formability of the duplicated feature made from POM (acetal) polymer with 20% added lead micropowders was compared to that of PP polymer with added nanopowders.

Kneading and granulation

A Z-blade kneader (Ray-E Manufacture Co., Tainan, Taiwan) operating at 35 rpm was used with a 650-mL mixing bowl. At the beginning of the kneading process, pure nanoceramic powders (SiO_2, TiO_2, and ZnO, with 10, 20, and 30%, respectively, of the total weight content of the polymer compound) were preheated to 175°C for 0.5 h in the kneader. PP plastic pellets were then added to the powders and kept at 175°C in the kneader. After kneading continued for 1 h, SA surfactant was added and the temperature of the kneader was reduced to 160°C and held for 30 min. The dough-type mixture was then granulated in the mixing bowl as the temperature of the bowl was reduced to 70°C for 24 h.

Quality evaluation

To illustrate the batch production process, one mold with four parts was manufactured using the custom-made microinjection machine. To study the filling behavior, the four cavities had to be completely filled with plastic compound during injection molding. The length (x) and width (y) of the cavities and parts denoted a, b, c, and d were measured with a coordinate measurement machine (Poli, Italy). The precision level of the measurements was 1 μm. The shrinkage (η_a) in part a could be calculated in terms of the average cavity length (l_a) and average part length (l_a') as follows:

$$\ell_a = (x_a + y_a)/2$$

$$\ell_a' = (x_a' + y_a')/2$$

$$\eta_a = \frac{\ell_a - \ell_a'}{\ell_a} \times 100\% \quad (1)$$

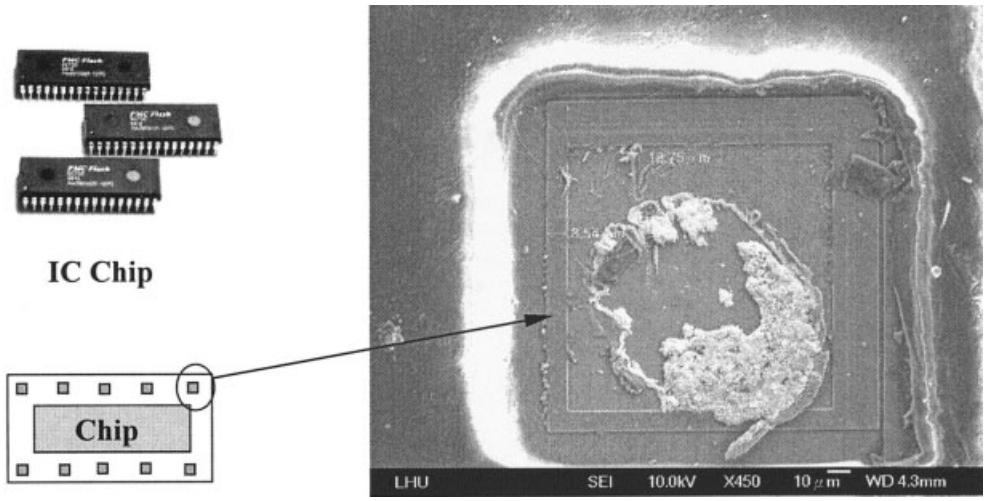

Figure 3 An SEM image of a weld spot in an integrated circuit chip.

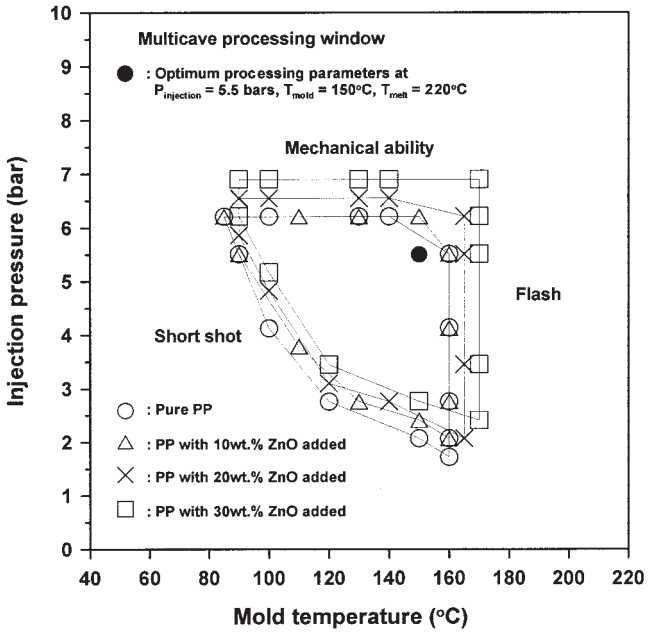

Figure 4 The processing window of the polymer with added nanopowders.

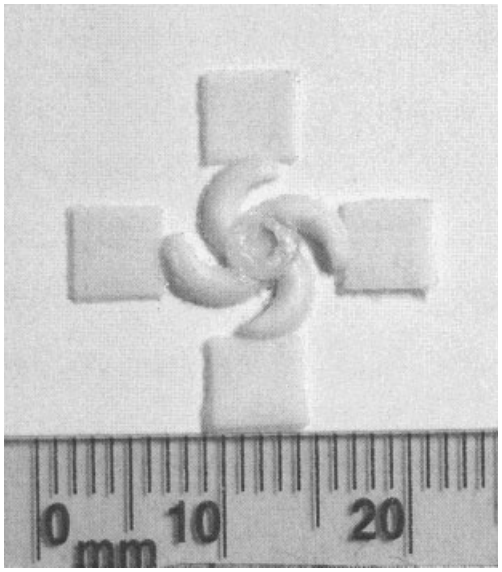

Figure 5 A photograph of the parts with 10% added ZnO nanopowders.

where x_a, y_a are the respective length and width of cavity a and x_a', y_a' are the respective length and width of part a. The shrinkage in parts b, c, and d was also obtained using eq. (1). The average shrinkage in each part was obtained from 10 specimens for every tested part.

RESULTS AND DISCUSSION

Filling behavior of one mold with multicavities

The processing window of the polymer with added nanopowders is shown in Figure 4. The formability of the polymer compound is better when the processing window is larger. The quality of the microparts is degraded when the processing parameters are out of the range of the window. Short-shot is produced in parts when processing is out of the leftward boundary of the window. Flash occurs in parts when processing exceeds the rightward boundary of the window. In addition, the mechanical ability of the custom-made machine is exceeded when processing jumps out of the top boundary of the window.

A photograph of the parts with 10% added ZnO nanopowder, using the above processing window, is shown in Figure 5. The photograph shows that the mold with four parts could be successfully manufactured by the custom-made injection machine. The average part weight is only 2.2 mg. The operating zone was shifted to the right when the weight content of the nanomaterials was increased. In other words, the injection pressure and mold temperature increased as the weight content of the nanomaterials increased. Parts with short-shot were formed when the forming pressure and mold temperature were low. The processing window of the polymer with 10% nanopowder was close to that of pure PP.

In the window, when the mold temperature was low, the forming pressure had to be increased to produce high quality parts. Theoretically, when the mold temperature is lower than the polymer melting tem-

TABLE I
Shrinkage of Polymer PP with Different Added Nanopowders

Powders	SiO_2 (%)	TiO_2 (%)	ZnO (%)
10%			
a	0.313	0.355	0.391
b	0.339	0.371	0.42
c	0.311	0.34	0.385
d	0.329	0.36	0.40
Ave.	0.323 (33.3)	0.358 (26)	0.399 (17.6)
20%			
a	0.249	0.261	0.289
b	0.264	0.291	0.301
c	0.242	0.236	0.27
d	0.253	0.28	0.292
Ave.	0.252 (47.9)	0.267 (44.8)	0.288 (40.5)
30%			
a	0.20	0.238	0.277
b	0.216	0.25	0.30
c	0.183	0.218	0.25
d	0.209	0.242	0.281
Ave.	0.202 (58.3)	0.237 (51)	0.277 (42.8)

The shrinkage of PP: a = 0.482, b = 0.511, c = 0.441, d = 0.502, Ave. = 0.484; a, b, c, d, cavity and part number of mold. The values in parentheses are the differences from polymer PP, e.g., 10%, SiO_2 = (0.484 − 0.323)/0.484 × 100% = 33.3%.

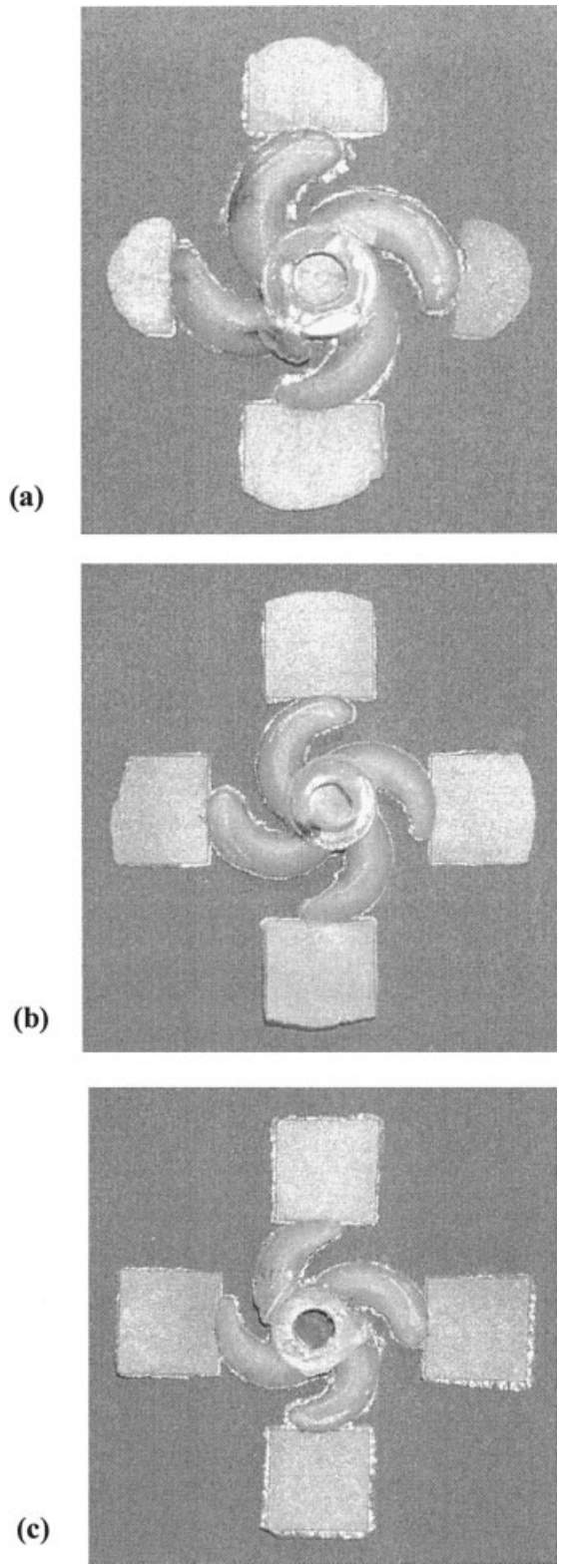

Figure 6 Short-shot tests with (a) 90, (b) 96, and (c) 100% molten polymers.

perature, a frozen layer will form as molten polymer flows into the cavities. In other words, high pressure will be needed to accelerate filling of the cavities with

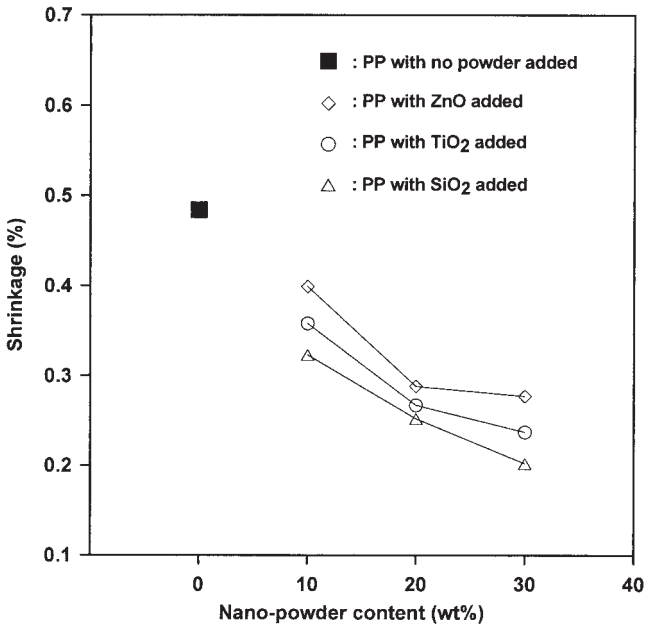

Figure 7 The shrinkage of polymer PP with different added nanopowders.

molten polymer before the polymer freezes. Thus, in micropart molding, high pressure and high mold temperature are needed to produce high quality parts.

In our experiments, optimum parameters, which were a 5.5-bar injection pressure, 150°C mold temperature, and 220°C melt temperature, were adopted in the tests described later.

Experimental observation in fabricating microparts

As shown in Table I, the amount of shrinkage of the four microparts in a mold varied slightly for each tested specimen. However, the shrinkage of the parts was always in the order $b > d > a > c$ for any powder. To further understand the reason for these results, short-shot experiments were conducted. A quantity of molten polymer PP from 90 to 100% was injected into

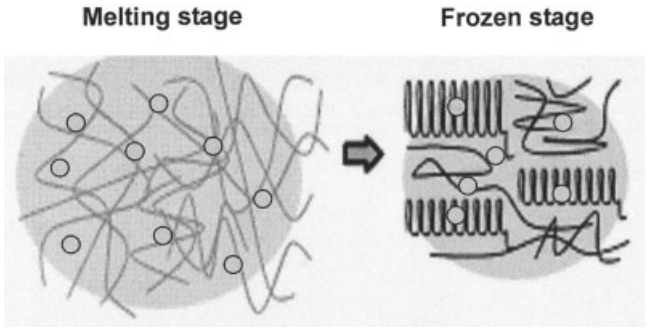

Figure 8 A diagram showing the activity and volume expansion of the molecules are retarded when nanopowders are added.

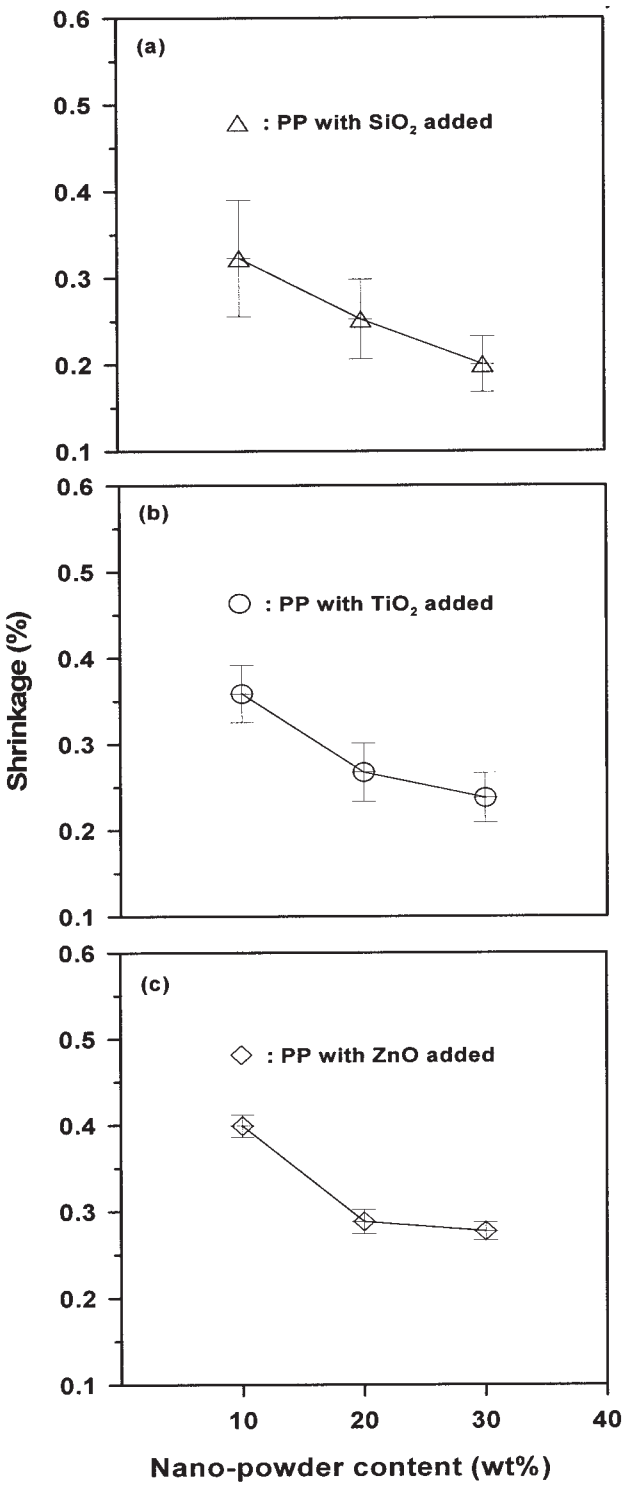

Figure 9 The error deviation of the shrinkage of polymer PP with different added nanopowders.

the cavities of the mold, as shown in Figure 6. Interestingly, the filled areas in the 90 and 96% molten polymer tests were in the order $b < d < a < c$, which was the opposite of the order of the shrinkage. The cavities were fully filled when 100% molten polymer was injected. The amount of shrinkage was lowest in part *c*, which exhibited the fastest formability during the short-shot tests. However, the amount of shrinkage was highest in part *b*, which exhibited the slowest formability during the short-shot tests.

The runner lengths for *a*, *b*, *c*, and *d* were 4.943, 4.991, 4.925, and 4.960 mm, respectively, as measured by means of the coordinate measurement machine. When the runner length was longer, the frozen layer

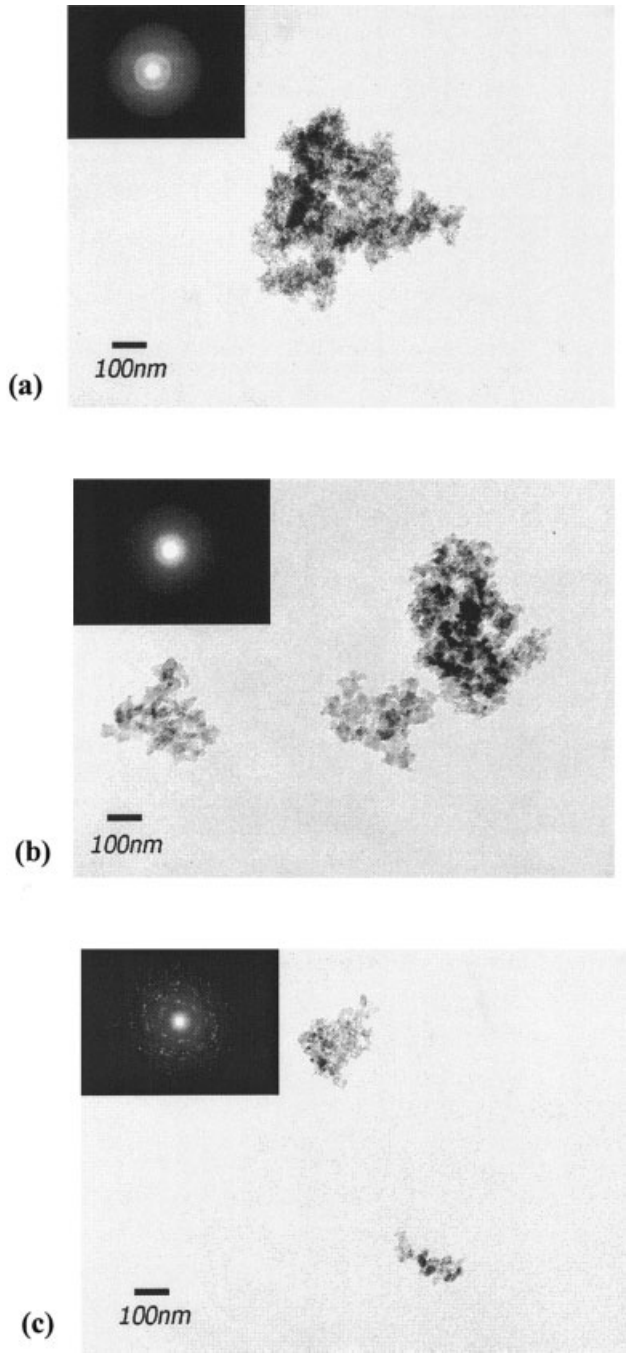

Figure 10 TEM micrographs for pure nanoparticles in the bright field image. The insert is a diffraction pattern and the centered dark fields are nanopowder images for (a) SiO_2, (b) TiO_2, and (c) ZnO nanoparticles.

formed earlier than it did when the runner length was shorter. A longer runner length with a frozen layer caused the cavity to fill more slowly with molten polymer. Then, the temperature difference between the mold and molten polymer increased, resulting in the largest amount of shrinkage in part *b*, which had the longest runner length. The runners and cavities of the mold were manufactured by means of electric discharge machining with a precision of 10 μm, resulting in slight variations in their dimensions. Thus, we suggest that microelectric discharge machining with a precision of 1 μm or the lithography (LIGA) process can be used to manufacture very accurate molds when precision microparts are formed.

Polymer shrinkage with varied percentages of nanoparticles added

The shrinkage results for polymer PP with different added nanopowders are shown in Figure 7 and Table I. The shrinkage was significantly reduced when the nanopowder weight content was increased for any powder. The polymer with 30% SiO_2 weight content exhibited the least shrinkage. The shrinkage of this polymer was decreased by 58.3% compared to pure PP. This clearly showed that the polymer with added nanoparticles effectively reduced the shrinkage. When the polymer was in the melting stage, nanoparticles reduced the activity of the molecules, resulting in significantly lower volume expansion of molecules, as shown in Figure 8. Then, crystallization of the molecules was retarded by nanoparticles during the frozen stage. Therefore, the shrinkage was reduced when nanoparticles were added to the polymer. The greater the powder content was, the less the shrinkage.

Figure 7 also shows that the polymer with added SiO_2 nanopowder exhibited the least shrinkage compared to the others. The polymer with added ZnO nanopowder exhibited the greatest shrinkage. SiO_2 (0.2 g/cm^3) had the lowest density, TiO_2 (0.25 g/cm^3) was next, and ZnO (0.3 g/cm^3) had the highest density. Under the same weight composition, the volume content of SiO_2 with the lowest density in the PP polymer was larger than that of the other two powders. In other words, more of the SiO_2 powder was distributed in the PP polymer. As explained in the previous paragraph, the SiO_2 with higher volume content exhibited the least shrinkage.

Micrograph analysis of nanoparticles distributed in polymer compound

Figure 9 shows the shrinkage deviations among 10 specimens for different nanomaterials. Large error deviations occurred in SiO_2 and TiO_2 nanopowders, as shown in Figure 9(a,b), but they were small in ZnO nanopowders, as shown in Figure 9(c). A possible

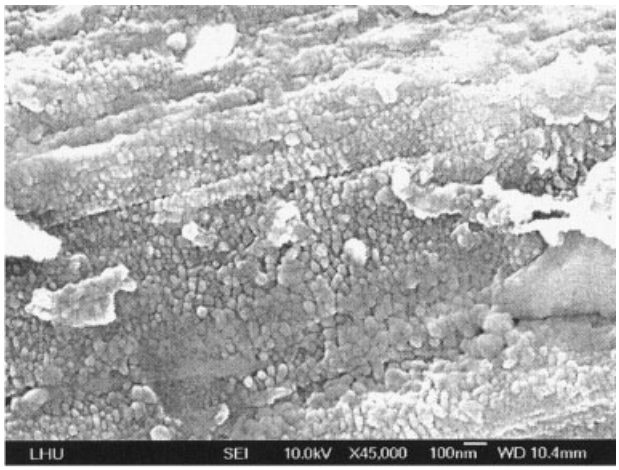

(a)

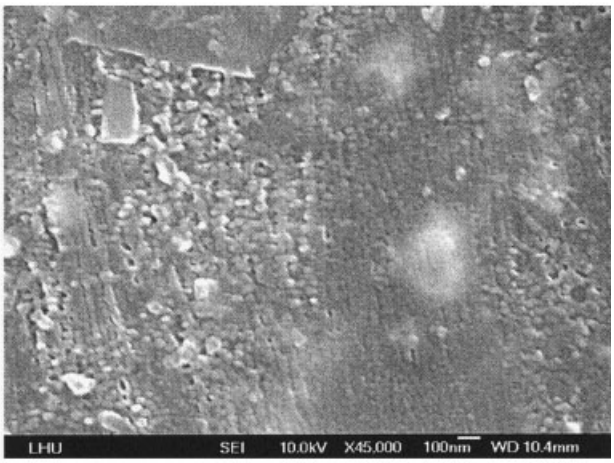

(b)

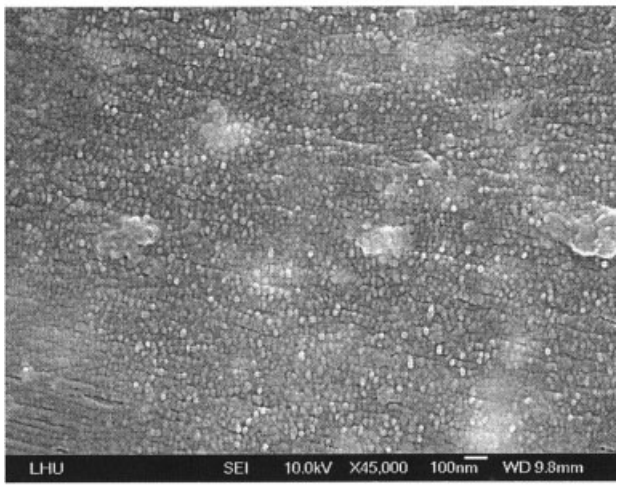

(c)

Figure 11 SEM images of the PP polymer with 20 wt % (a) SiO_2, (b) TiO_2, and (c) ZnO nanoparticles.

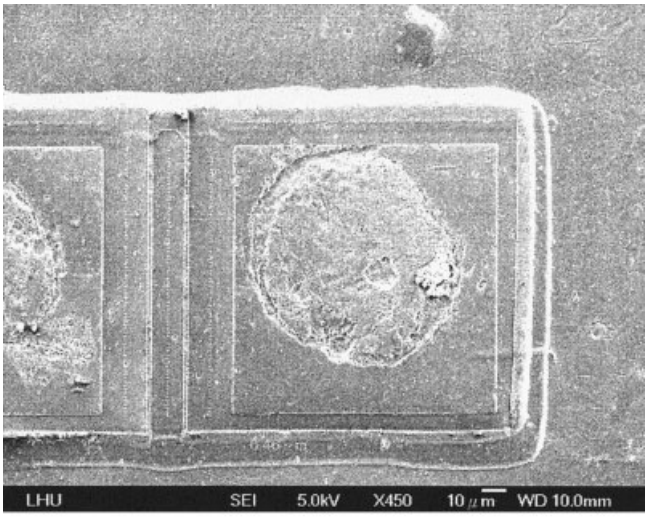

(a)

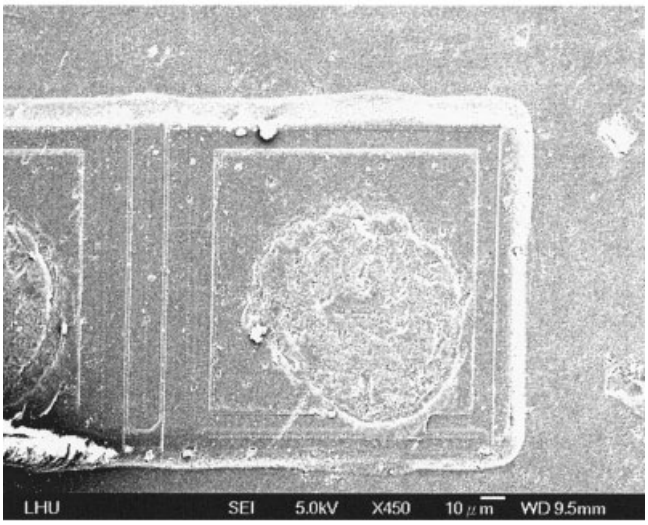

(b)

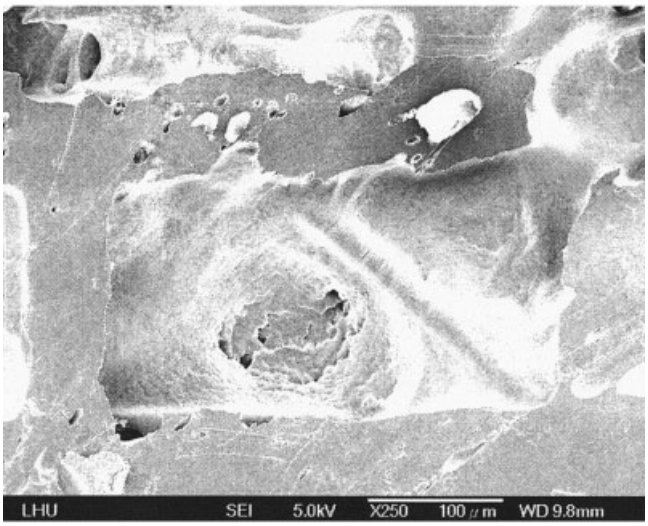

(c)

reason could be that the nanoparticles were not uniformly distributed in the polymer compounds containing SiO_2 and TiO_2 nanopowders. In order to understand the reason, a Jeol transmission electron microscopy (TEM) microscope was used to analyze the morphologies of the pure nanoparticles. The micrographs for different nanoparticles are shown in Figure 10. The bright field image with an inserted diffraction pattern is shown in the left-top corner, and the dark center field in each micrograph is the nanopowder image.

The SiO_2 nanoparticles were heavily agglomerated [Fig. 10(a)]. The primary particles with sizes <10 nm formed connections to the neighboring particles at the neck area. The dark center field image of the nanoparticles showed uniform contrast through every SiO_2 particle. In addition, the ring diffraction pattern revealed amorphous characteristics (see the insert diffraction pattern). Similar to SiO_2 particles, the TiO_2 nanoparticles revealed amorphous characteristics and had some degree of agglomeration, as shown in Figure 10(b). The size of the primary particles was about 20–30 nm. They strongly showed that both SiO_2 and TiO_2 nanoparticles were difficult to blend with polymers, resulting in the agglomeration that existed in the polymer compound. The effect was greater for SiO_2 than for TiO_2. Large error deviations between specimens were thus induced because the nanoparticles were not uniformly distributed in the polymer compound.

On the contrary, the ZnO nanoparticles with slight agglomeration, as shown in Figure 10(c), consisted of 10–20 nm primary particles that were crystalline, as shown by the electron diffraction pattern. The error deviations between the specimens were small because the nanoparticles were easily distributed in the polymer compound. Furthermore, the ZnO nanoparticles with higher density and better crystals than the other two powders thus exhibited greater shrinkage because there was less agglomeration. The higher the density was, the greater the shrinkage and the better the powder dispersion.

To further understand the reason for these results, scanning EM (SEM, JSM-6500F) images of the polymer compound with 20% of the total weight being added SiO_2, TiO_2, and ZnO are shown in Figure 11. The SiO_2 nanoparticles with 20% added weight content created the most serious agglomeration in the polymer compound, as shown in Figure 11(a), with the TiO_2 nanoparticles being next, as shown in Figure 11(b). Conversely, the ZnO nanoparticles with 20% weight con-

Figure 12 SEM images of a microfeature for one mold with one cavity: (a) PP with 20% ZnO nanopowder, (b) PP with 30% ZnO nanopowder, and (c) POM with 20% Pb micropowder.

tent were uniformly distributed in the polymer compound, as shown in Figure 11(c). These results were similar to the previous TEM analyses.

In addition, in a previous study[23] we conducted a wear test with a polymer compound with SiO_2, TiO_2, and ZnO nanoparticles. The experiments showed that the weight loss of the polymer with 20% ZnO nanoparticles was only 0.8% because the particles were uniformly distributed in the polymer compound. However, the weight losses of the polymer compound with 20% SiO_2 and 20% TiO_2 nanoparticles were 12 and 3%, respectively, because the particles agglomerated extensively in the polymer compound.

Formability of microfeatures

Four parts in a mold were successfully manufactured using a custom-made microinjection machine when nanopowders were added to the polymer. This proved that in batch production manufacturing with microinjection molding, polymers with added nanoparticles can be used to produce parts from multiple-cavity molds.

To further understand how the microfeatures with added nanopowders were formed, the boundaries of an 8.54 $\times$ 18.75 μm weld spot in an IC chip, which was taken from a scrapped computer, were selected for duplication, as shown in Figure 3. The required injection pressure and mold temperature were lower because only one micropart was formed in a mold.

SEM images of duplicated microparts with 20 and 30% ZnO nanopowder are shown in Figure 12(a,b). The edges of the duplicated microfeatures were well defined. In other words, the plastic compound with added nanopowders easily filled the microcavity. However, nanoparticles agglomerated in the PP polymer, similar to the previous results obtained when the powder content exceeded 20%. The dimensions of the plastic compound with 20 and 30% powder content were 6.46 $\times$ 7.92 and 7.92 $\times$ 18.33 μm compared to those of the IC chip, which were 8.54 $\times$ 18.75 μm. Shrinkage of the duplicated feature with 30% nanopowder was less than that of the duplicated part with 20% nanopowder. This result was similar to that discussed previously. Thus, microfeatures were successfully manufactured when a plastic compound with nanopowder was added during the microinjection molding process.

The SEM image in Figure 12(c) shows a duplicated feature made from POM polymer with 20% added Pb micropowder. The image shows that the cavity was not successfully filled with polymer compound. This is because the Pb fillers with a diameter of 10 μm and a length of 10 to 30 μm were as large as the microfeature that was molded in this study. These results agree with those of Schneider and Maier.[20] Thus, nanodiameter fillers are the best choice for microinjection molding.

CONCLUSION

Based on this study on the applications of nanomaterials in microinjection molding, the following conclusions can be drawn:

1. One mold with four parts and microfeatures were successfully manufactured using a custom-made injection machine when nanopowders were added to the polymer.
2. The injection pressure and mold temperature had to be increased as the nanopowder weight content increased. Short-shot formed in parts when the forming pressure and mold temperature were too low. The formability of the polymer with 10% nanopowder was similar to that of pure PP.
3. Shrinkage was significantly reduced when the nanopowder content was increased. The polymer with 30% SiO_2 weight content exhibited the least shrinkage. When nanopowders were added, the activity and volume expansion of the molecules were retarded during the melting and frozen stages, thus reducing shrinkage.
4. The ZnO nanoparticles with higher density and better crystals than the other two powders thus exhibited greater shrinkage because there was less agglomeration. The higher the density was, the greater the shrinkage and the better the powder dispersion.
5. TEM and SEM showed SiO_2 and TiO_2 nanoparticles were heavily agglomerated in the polymer compound, resulting in large shrinkage deviations between specimens and a decrease in wear abrasion. However, ZnO nanoparticles were uniformly distributed in the polymer compound, resulting in small shrinkage deviations and increasing wear abrasion.
6. The edges of the duplicated IC microfeatures with 20 and 30% powder content were well defined. The plastic compound with added nanopowders easily filled the microcavity. However, in the case of the part duplicated using the POM polymer with 20% Pb, the cavity was not successfully filled with polymer compound. This is because the Pb fillers with a diameter of 10 μm and a length of 10–30 μm were as large as the micropart that was molded in this study.

The authors express their appreciation for the financial support of this research provided by the National Science Council of Taiwan.

References

1. Ruprecht, R.; Benzler, T.; Hanemann, T. Microsyst Technol 1997, 4, 28.
2. Michaeli, W.; Spennemann, A.; Gartner, R. Microsyst Technol 2002, 8, 55.
3. Hill, S. Mater World 2001, June, 24.
4. Michaeli, W.; Rogalla, A.; Ziegmann, C. Kunststoffe 1999, 89, 80.
5. Macintyre, D.; Thomas, S. Microelectron Eng 1998, 41, 211.
6. Weber, L.; Ehrfeld, W. Micro-Molding-Processes, Moulds, Applications, Kunststoffe Plastic Europe, Oct. 1998, Vol. 88, pp 1791–1802.
7. Ruprecht, R.; Hanemann, T.; Piotter, V.; Haubelt, J. J Proc Int Soc Opt Eng 1995, 2639, 146.
8. Weber, L.; Ehrfeld, W.; Freimuth, H.; Lacher, M.; Lehr, H.; Pech, B. J Proc Int Soc Opt Eng 1996, 2879, 156.
9. Rogalla, A.; Michaeli, W. Proceedings of the 55th Annual Technical Conference of the Society of Plastics Engineers, Toronto, Canada, 1997, pp 365–368.
10. Kukla, C.; Loibl, H.; Detter, H. Micro-Injection Moulding, The Aims of a Project Partnership, Kunststoffe Plastic Europe, Sep. 1998, 51, 1331–1336.
11. Larsson, O.; Ohman, O.; Billman, A.; Lundbladh, L.; Lindell, C.; Palmskog, Proceedings of the 1997 International Conference on Solid-State Sensors and Actuators, Chicago, IL, 1997, pp 1415–1418.
12. Bourdon, R.; Schneider, W. Kunststoffe, 1998, 88, 1791.
13. Despa, M. S.; Kelly, K. W.; Collier, J. R. Microsyst Technol 1999, 6, 60.
14. Fasset, J. Plast Eng 1995, 51, 35–37.
15. Merze, L.; Rath, S.; Piotter, V.; Ruprecht, R.; Ritzhaupt-Kleiss, J.; Hausselt, J. Microsyst Technol 2002, 8, 129–132.
16. Gietzelt, T.; Piotter, V.; Jacobi, O.; Ruprecht, R.; Hausselt, J. Adv Eng Mater 2003, 5, 139–145.
17. Su, B.; Button, T. W.; Schneider, A.; Singleton, L.; Prewett, P. Microsyst Technol 2002, 8, 359.
18. Rota, A.; Duong, T. V.; Hartwig, T. Microsyst Technol 2002, 8, 323–325.
19. Piotter, V.; Gietzelt, T.; Merze, L. Micro Powder Injection Moulding of Metals and Ceramics, Sadhana, 2003, 28(Parts 1&2), pp 299–306.
20. Schneider, C.; Maier, G. Kunststoffe, 2001, 91, 82.
21. Yang, S. Y.; Nian, S. C.; Sun, I. C. Int Polym Proc 2002, 17, 355.
22. Eberle, H. Micro-Injection Moulding, Mould Technology, Kunstoffe Plastic Europe, Sep. 1998, Vol. 88, pp 1344–1346.
23. Huang, C. K.; Chiu, S. W. Compos Part A: Appl Sci Manufac 2005, to appear.